Hyperfine Interact (2018) 239: 14
https://doi.org/10.1007/s10751-018-1490-6

Mossbauer spectroscopy study of $Fe@ZrO_2$ nanocomposites formation by MA SHS technology

Tatiana Kiseleva[1] · Alexey Letsko[2] · Tatiana Talako[2] · Svetlana Kovaleva[3] · Tatiana Grigoreva[4] · Alla Novakova[1] · Nikolay Lyakhov[4]

Published online: 5 February 2018

Abstract Particles with core-in-shell structure $Fe@ZrO_2$ were synthesized by step-by-step technology including formation of mechanically pre-activated (MA) precursors with Fe/Zr and Fe_2O_3/[Fe/Zr] composite structures formation following by Self-Propagated High temperature synthesis (SHS). Mossbauer spectroscopy, Transmission and Scanning electron Microscopy have been performed to study the peculiarities of local structure and its evolution through the sequential synthesis steps via various milling periods and reagent compositions. The exact conditions for iron core in oxide shell $Fe@ZrO_2$ structure formation with promising functionality has been established.

Keywords Mossbauer spectroscopy · Nanocomposites · Core-in-shell · Mechanosynthesis · Self propagated high temperature synthesis · Iron · Zirconia

1 Introduction

The core-in-shell nanomaterials and nanostructures have gained considerable attention and have become an important research area due to their potential applications in industry and

This article is part of the Topical Collection on *Proceedings of the International Conference on the Applications of the Mössbauer Effect (ICAME 2017), Saint-Petersburg, Russia, 3–8 September 2017* Edited by Valentin Semenov

✉ Tatiana Kiseleva
Kiseleva.TYu@gmail.com

[1] Department of Physics, Moscow M.V. Lomonosov State University, Moscow, Russia

[2] Institute of Powder Metallurgy NAS, Minsk, Belarus

[3] United Institute of Mechanical Engineering, Minsk, Belarus

[4] Institute of Solid State Chemistry and Mechanochemistry RAS, Novosibirsk, Russia

medicine [1]. Up to now it is found that particles with nanoshells can be synthesized practically with the help of any materials, like semiconductors, metals and insulators. Among these materials the particles with ferromagnetic/antiferromagnetic structure, containing iron core covered by dielectric shell exhibits very interesting electrical, optical and magnetic properties [2, 3]. Core-in-shell particles can be assembled and further utilized to design components of composite materials.

Fe (*Iron*) particles covered by ZrO_2 (*Zirconia*) shell containing composite materials are of great interest for usage as functional coatings, catalysts, for medical and biotechnological purposes [4]. Due to good insulating properties, chemical inertness, wear resistance, high fracture toughness of ZrO_2 for magnetic particles encapsulation extends applying of composite material in improvement of special composite technologies.

Numerous techniques (like sol-gel, electron-beam evaporation, chemical precipitation, hydrothermal methods and by combustion) developed for synthesize incapsulated particles in most cases involve multistep synthesis procedure [5–9]. The usage of self-propagating high temperature synthesis on mechanically pre-activated powdered precursors for this purposes with finding of the optimal exact synthesis conditions has been recently proposed by our collaborative group [10].

Self-propagating high-temperature synthesis (SHS) of powdered composites is based on the exothermal reaction between several components (oxides and metals, for example) [11, 12]. It can proceed in a combustion mode after local initiation of the process. The preliminary mechanical activation (MA) of the powdered reactive mixtures is considered to be efficient for purposefully influencing the structure of the reactive powder batch and SHS parameters that allow the mechanisms of materials phase and structure formation to be regulated during synthesis. Recently we have studied mechanical interactions in oxide–active metal systems like CuO–Me [13, 14], FeO(Fe_2O_3)-Me (Me are Al, Ti, and Zr) [15] that have shown that composite materials synthesis in the systems via the above methods is very complex and depends on a number of parameters (compositions, depth of interaction, dispersity etc). Oxide reduction is high exothermic and passes usually in the thermal explosion mode, in particular for the reaction $2Fe_2O_3+3Zr \rightarrow 3ZrO_2+4Fe$ ($\Delta H = -1655\ \kappa$J/mol). It was shown that double-step mechanical activation including step of Cu–Me, Fe-Me (where Me are Ti and Zr) composite particles precursors synthesis, following its subsequent admixture with oxides with subsequent mechanosynthesis of the triple CuO–Cu/Me or Fe_2O_3-Fe/Me mechanocomposites allows to avoid the intensive dispersion of materials during SHS. Premilling of highly reducing metal with less active one allows the dilution of the termite mixture reactivity and permits to translate reaction from the thermal explosion into the burning mode. The control of reaction rates is possible also through adjusting the degree of interaction between components during the mechanical activation as at the first step in bimetallic mixtures of Cu–Me or Fe-Me (Me: Ti, Zr), as at the second step of CuO–Cu/Me or Fe_2O_3-Fe/Me premilling interaction. It is necessary to manage the degree of interaction on the contact surface between the particles in reacting mixture. The result significantly influences the degrees and depth of interaction when final morphology and structure of nanocomposites will be formed. Thus it is possible to find the exact conditions of the desired material structure formation, even functional core-in-shell structure, by selecting the suitable composition of the reacting mixture and regulating the structure and morphology of the material at each stage of mechanical interaction.

In this study iron encapsulated by zirconia Fe@ZrO_2 powdered nanocomposites was the aim of the step-by-step synthesis from mechanically pre-activated precursors of Fe/Zr and Fe/Zr/Fe_2O_3 compositions combining with subsequent self-propagated high temperature synthesis (SHS). The presence of iron as constituent component of complex composite

structures allowed us to study the influence of the local structure formation at each step of synthesis on the resulting nanostructure using possibility of Mossbauer spectroscopy [16].

2 Experimental

2.1 Sample preparation

Following initial materials were used: carbonyl iron (*Fe*) (iron content >97.6 wt. %, according to Russian standard GOST 13610-79), iron oxide (Fe_2O_3) (Russian standard TC 6-09-5346-87), zirconium (*Zr)* (Russian standard M-41). The mechanical activation was carried out in AGO-2 high energy ball mill under Ar-atmosphere. The volume of the steel drum was 250 cm^3, diameter of steel balls was 5 mm, and the ratio of a mass of balls to a mass of the prepared material was 20:1; the rate of the drum rotation around the common axis was ∼1000 rep/min).

We performed *step-by-step synthesis* of composite powdered materials consisted of the following sequential stages:

I-step: mechanical activation (MA) during 4 min of the 80Fe20Zr (numbers are weight percents unless stated otherwise) powder mixture with the formation of [Fe/Zr] double mechanocomposites;
II-step: the mechanical activation (MA) of synthesized [Fe/Zr] (13.7 g) double composite powders with Fe_2O_3 (1.6 g) during 4 min and 2 min to obtain multicomponent Fe_2O_3/[Fe/Zr] composite powder precursor.
III-step: selfpropagating high temperature synthesis (SHS) in argon atmosphere on multicomponent composites synthesized in the previous two steps. The sample was set on fire by the tungsten coil heated by the current. Temperature and combustion rate were estimated via a thermal couple method (chromel–alumel thermal couples with a diameter of ≈0.2 mm) using an external twin-channel 24-bit analog-to-digital converter ADSC24-2T.

Additional mechanochemical synthesis was performed in powder mixture with composition Fe_2O_3 (6.4 g) +Zr (2.6 g) calculated to realize full mechanically induced oxide reduction reaction.

No contamination of the material occurred from the applied mill drum and the grinding balls with the used activation time, as was shown in [17].

2.2 Samples characterization

Morphology and particle sizes at different steps of synthesis were studied by transmission electron microscopy (TEM) on a LEO 912 AB microscope at 0.34 nm resolution in bright-field and dark-field imaging modes. Dark-field images were collected in (110) reflection of α-Fe.

Scanning electron microscopy (SEM) images were recorded on MIRA\TESCAN high-resolution scanning electron microscope equipped with a micro-X-ray spectral analysis (MXRSA) attachment. Image analysis was done using ImageJ software [18].

The local structure of the composites at each synthesis step was probed by Mossbauer spectroscopy. Mossbauer spectra were recorded using MS1104 Em ("*Kordon*") spectrometer at the temperatures of 300 and 80 K in a low-temperature cryostat in transmission geometry. $Co^{57}(Rh)$ was used as gamma-radiation source. Analytical processing of spectra was performed using Univem MS software [19].

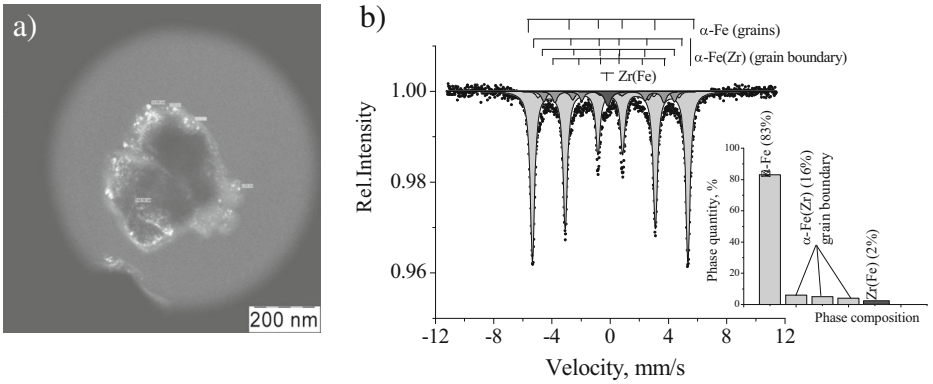

Fig. 1 TEM image in dark-field mode of the typical particle (**a**), Mossbauer spectrum (**b**), phase composition diagram (in inclusion) of the [Fe/Zr] composite particles, obtained at 4 min of MA

3 Results and discussion

Zirconium and iron have high melting points and low mutual solubility [20] (∼0.02 at% Fe in α-Zr at 700 °C, and 0.1 at% Zr in α-Fe and 0,2 at% in γ-Fe) Iron is known to be more plastic than zirconium. So a rapid milling of zirconium and its distribution in the composite mixture favors formation of composite [Fe/Zr] particles, as obviously seen from the dark-field TEM image (Fig. 1a). A composite particles with sizes of ∼300–500 nm have a (*bcc*)Fe structure and (*fcc)*Zr nanoscale inclusions (the bright spots in the dark-field pattern) with sizes of 6–14 nm.

Figure 1b displays the Mossbauer results for [Fe/Zr] mechanical nanocomposite. It exhibits complex spectral profile that combines subspectra of different iron local structures. These subspectra can be interpreted in the known model used for nanocrystalline materials that distinguish different structural components [21–23]. According to this model a spectrum of nanocrystalline iron obtained by intensive mechanical treatment may be described by superposition of the components corresponding to the Fe-grains ($H_{eff} = 330$ kOe) with long-range order, interfacial/grain boundaries component, where local atomic coordination differs from volumetric and the effects of their disordering are reflected in line broadening due to diversity of iron surroundings caused also by the presence of Zr in this disordered zone ($H_{eff} = 301$, 278, and 232 (±3 kOe), Table 1). The grain boundary fraction should rise rapidly when grains became less than 20 nm [24] and will give a greater contribution to the spectrum. Nonequivalent iron positions are highlighted by the spectral components with reduced H_{eff} values if the iron particles contain small zirconium particles, as it is observed in Fig. 1. This is due to the modified environment of iron atoms in the local zones of the particle.

A single component of the spectrum with parameters $\delta = -0.08$ mm/s, corresponds to the αZr(Fe) phase (the dilute solid solution of iron in zirconium [25]).

As it was shown recently [28–30], the mechanical activation of Fe_2O_3 mixtures with reducing metals (for example, Al and Ti) can occur in heating explosion mode, leading to both complete reduction of iron oxide and partial formation of composite structures containing metal oxides, depending on mutual concentration and activation energeticity. The activity of metal as a reductant and energeticity of mechanical activation favors the rates and the degree of passing mechanoactivating reaction. The dilution of mixtures by inactive

Table 1 Mossbauer spectra parameters (H_{eff}-hyperfine field, δ- isomer shift, ΔQ- quadruple shift, G-linewidth, S-relative area) for studied samples

Sample	Mossbauer spectra parameters							Phase composition
	Milling time, min	SHS	Heff, kOe	δ, mm/s	ΔQ, mm/s	G, mm/s	S, %	
[Fe/Zr] bm	4		330	0.00	0.01	0.35	83	α-Fe
			301	0.08	−0.04	0.40	3	α-Fe(Zr)(grain boundary)
			278	−0.02	−0.09	0.40	5	
			232	0.08	−0.12	0.45	6	
				−0.08		0.45	3	Zr(Fe)
Fe_2O_3+Zr			330	0.00	0.01	0.28	57	α-Fe
				0.33	0.80	0.32	5	ZrO_2/Fe^{3+}
				0.94	0.85	0.60	32	ZrO_2/Fe^{2+}
				−0.10		0.48	6	Zr(Fe)
Fe_2O_3/[Fe/Zr]	4		515	0.39	−0.25	0.35	7	α-Fe_2O_3
			330	0.00	0.0	0.36	70	α-Fe
			301	0.04	−0.10	0.40	5	α-Fe(Zr)(grain boundary)
			278	−0.02	−0.09	0.40	7	
			232	0.09	−0.11	0.40	7	
				−0.08		0.50	4	Zr(Fe)
Fe_2O_3/[Fe/Zr]	4	SHS	512	0.35	−0.16	0.45	2	α-Fe_2O_3
			492	0.21	0.01	0.51	3	Fe_3O_4
			455	0.29	0.56	0.71	8	
			330	0	0	0.31	77	α-Fe
			210	0.20	0.04	0.45	6	Fe_2Zr
				0.33	0.80	0.32	2	ZrO_2/Fe^{3+}
				−0.07		0.40	2	Zr(Fe)
Fe_2O_3/[Fe/Zr]	2		515	0.39	−0.25	0.35	9	α-Fe_2O_3
			330	−0.00	0.01	0.35	74	α-Fe
			301	0.11	−0.20	0.40	6	α-Fe(Zr)(grain boundary)
			278	−0.02	−0.09	0.40	6	
			232	0.08	−0.22	0.41	4	
				−0.08		0.33	2	Zr(Fe)
Fe_2O_3/[Fe/Zr]	2	SHS	512	0.35	−0.16	0.45	2	α-Fe_2O_3
			492	0.21	0.01	0.51	3	Fe_3O_4
			455	0.29	0.56	0.71	8	
			330	0	0	0.31	77	α-Fe
			210	0.20	0.04	0.45	6	Fe_2Zr
				0.33	0.80	0.32	2	ZrO_2/Fe^{3+}
				−0.07		0.40	2	Zr(Fe)

to the reduction metals (in particular, iron) allows controlling the rates and the mechanisms of interaction [31, 32]. In the series of metal activity, zirconium is a high reducing metal. Phase composition derived from Mossbauer spectrum (Fig. 2, Table 2) of the sample after

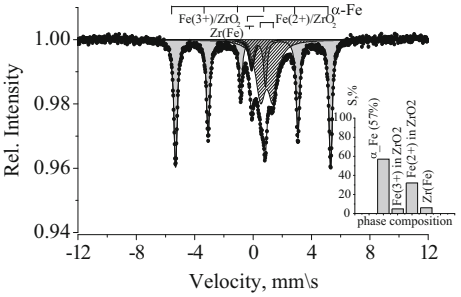

Fig. 2 Mossbauer spectrum of the full reduction result in MA mixture of Fe_2O_3 (6.4 g) +Zr (2.6 g)

Table 2 Elemental analysis of MA Fe_2O_3/[Fe/Zr] sample from zones, marked at Fig. 3c

Zone	Fe, %	Zr, %	O, %
Spectrum 1	10.1	69.9	20.0
Spectrum 2	98.6	0.0	1.4
Spectrum 3	8.3	78.6	13.1
Spectrum 4	98.6	0.2	1.6
Spectrum 5	53.1	22.1	24.8
Spectrum 6	84.1	8.7	7.1
Spectrum 7	63.2	15.2	21.6

the mechanical activation of Fe_2O_3 (6.4 g) and Zr (2.6 g) mixture for 1 min, which is displayed on the diagram, reveals that the result of the interaction is a composite containing particles with *bcc*-Fe (a component with magnetic ultrathin splitting $H_{\text{eff}} = 330$ kOe (75%) (Fig. 2, shown in gray color), ZrO_2 zirconium oxide with two- and three-valent iron (a doublet component (33%) —Fe(2+)/$ZrO_2$with parameters $\delta = 0.94$ mm/s, $\Delta = 0.85$ mm/s, and Fe(3^+)/ZrO_2 with parameters $\delta = 0.33$ mm/s, $\Delta = 0.80$ mm/s) [33, 34]. A spectrum also contains a nonmagnetic singlet with parameters which correspond to Zr(Fe) (3%) phase (unreacted zirconium fraction).

When performing the mechanical activation of Fe_2O_3 with [Fe/Zr] composite particles instead of pure zirconium particles, the interacting mixture is diluted by a poor reductant metal, namely, iron. The dilution enables us to regulate the process of particle grinding and manage the rates of interaction with iron oxide dividing the local area of active interaction.

SEM images (Fig. 3a,b) reveal that large composite particles are characterized by several heterogeneity scales. An elemental analysis (Table 2) of the local zones (designated in Fig. 3c), reveals that particles with a size of 3–4 μm (with a round shape, almost unformed and deformed after MA) that are the pristine iron; small particles were mainly located at the grain boundaries of metallic particles and the zones enriched with zirconium (the light zones) have small sizes.

The SEM image highlights areas around metallic particles with reduced heterogeneity scale. Inside these layers, it shows thin zones with a mixed color, which can testify to the subtle mixing of components and/or some mechanochemical interaction, since zirconium is an active reductant.

A partial oxide reduction fter the mechanical activation of Fe_2O_3 with [Fe/Zr] was proven by X-ray diffraction (not shown): in these samples after 4 min mechanical activation (in addition to reflexes from Fe_2O_3 (R-3c) hematite and α-Fe (Im-3m)), reflexes of tetragonal

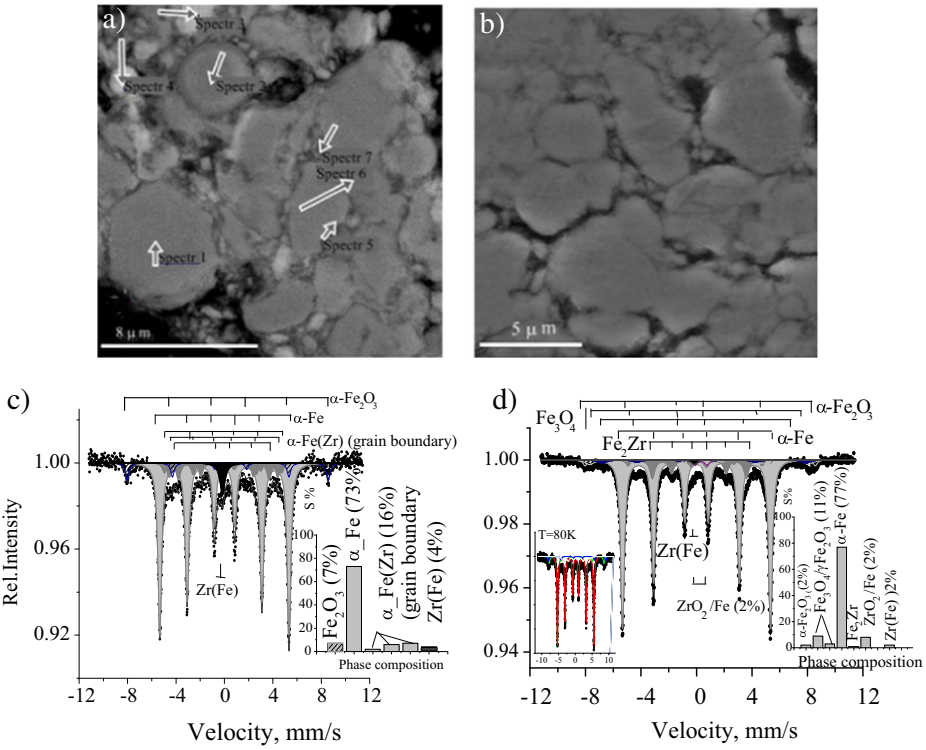

Fig. 3 SEM images and Mossbauer spectra of the samples after the second MA stage of Fe_2O_3/[Fe/Zr] (x = 4 min) (**a**, **c**) and the results of SHS on this precursors (**b**, **d**), derived phase composition (shown in bar diagrams)

ZrO_2 zirconium dioxide (*P*42/*nmc*) were identified [15]. The tetragonal phase of zirconium dioxide is metastable and its stabilization is possible by Fe ions [33]. Mossbauer results of 4 min interaction between components in powder mixture Fe_2O_3/[Fe/Zr] is shown in Fig. 3a.

The analytical processing of spectra revealed that if the reduction reaction passes during MA, it is not too active. Herewith, the active grinding of iron particles is observed. If we compare the ratio of the quantity of *bcc* iron particles grains to the number of disordered state on the iron grains surfaces and interfaces - $S(\alpha\text{Fe})/S(\alpha\text{Fe(Zr)}$—we see that it is reduced in relation to [Fe/Zr] composite, characterizing the increase in the fraction of the atoms on the particle surface and interfaces. All this is accompanied by Mossbauer line broadening (Table 1). Figure 3b, d depicts Mossbauer spectra and SEM images of SHS composites based on this mechanically synthesized precursors. The main spectral component again belongs to α-Fe. Its spectral line narrowing testifies the increasing particle sizes. The spectrum consist of several components indicating alloying during SHS process: sextet with parameters corresponding to Fe_2Zr phase ($H_{\text{eff}} = 220$ kOe) [25–27], doublets with parameters being characteristic to Fe^{3+} ions in ZrO_2 [34] and Zr(Fe) [25]. The interaction in the mixture is also proven by the changed parameters of the components associated with the oxide component. An analysis of spectral parameters revealed the presence of α-Fe_2O_3 phase (a sextet with parameters $H_{\text{eff}} = 515$ kOe) in the spectra. The sextet with parameters being close to both Fe_3O_4 and γ-Fe_2O_3 is also resolved in the spectra. It is worth

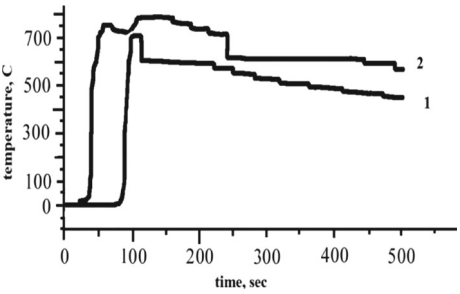

Fig. 4 The comparison of SHS thermograms for the samples with precursors Fe_2O_3/[Fe/Zr] 4 min (*1*) and Fe_2O_3/[Fe/Zr] 2 min (*2*)

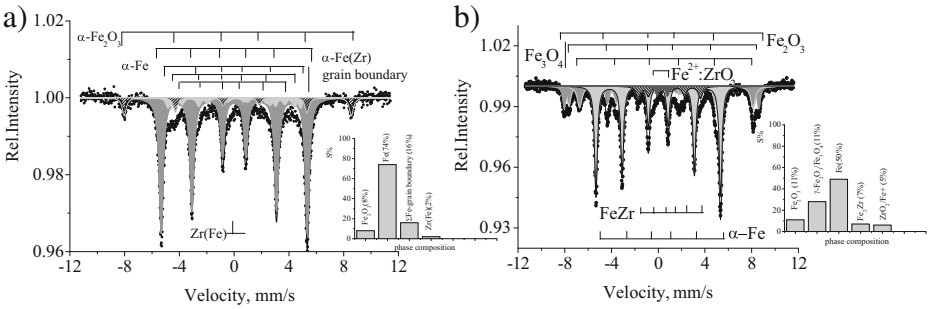

Fig. 5 Mossbauer spectra of Fe_2O_3/[Fe/Zr] mixture mechanically activated during min (**a**) and the result of SHS on this precursor (**b**), diagrams of phase composition (**c**, **d**), correspondingly

mentioning that X-ray diffraction does not allow Fe_3O_4 and γ-Fe_2O_3 to be distinguished. Mossbauer parameters of these oxides in the bulk materials are different, which allows uniquely to determine the oxide structure. Nevertheless, in the case of decreasing particle sizes, structural defectiveness, and the nonstoichiometry caused by the synthesis method, a typical Mossbauer spectrum of Fe_3O_4 (γ-Fe_2O_3) takes the form of the distributed ultrathin magnetic fields, which leads to uncertainty in the structure identification.

It is also possible that one result of the mechanochemical reduction of hematite is the heterogeneous mixture containing a set of structural states with various stoichiometry. In order to reveal the type of these oxides, Mossbauer spectrum was recorded at a temperature of $T = 80$ K. Figure 3b on the left insert proves the presence of γ-Fe_2O_3. The additional component is most likely to arise due to size effects, defectiveness, and even Zr replacement.

Recently we studied that the increase of duration of mechanical interaction in mixture of the Fe_2O_3 /[Fe/Zr] leads to the mechanochemical synthesis of intermediate intermetallic phases and oxides and subsequent SHS synthesis using these precursors result in the changes in the morphology of the product from less to more homogeneous. To obtain Fe particles surrounded by oxide components it seems to be likely required separating local interaction areas of the components and transferring interaction only to the surface of iron particles.

To change the velocity of the SHS process we performed the reducing of the period of [Fe/Zr] composite mechaical interaction with Fe_2O_3 in twice (from 4 to 2 min).

The comparison of the thermograms of the SHS processes obtained on the precursors Fe_2O_3/[Fe/Zr] 4 min (Fig. 4(1)) and Fe_2O_3/[Fe/Zr] 2 min (Fig. 4(2)) testify that the rate of temperature rise of almost the same in this two samples, but ignition time and the maximum

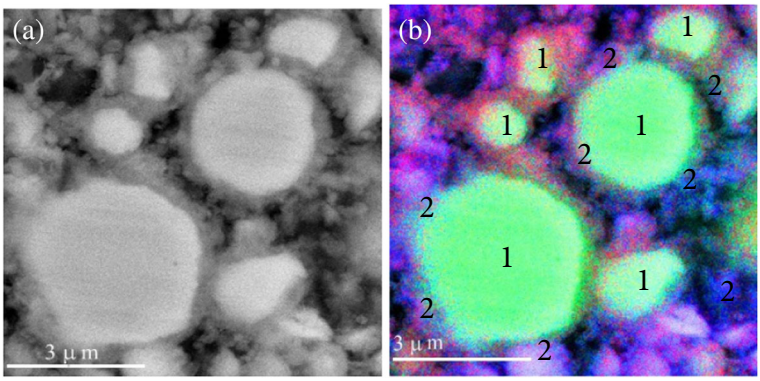

Fig. 6 SEM images of the SHS composite formed on Fe_2O_3/[Fe/Zr] 2 min: morphology (**a**) and elements distributions (**b**) Fe-green color (1), Zr-Fe-O oxides- blue color (2)

heating temperature are quite different: 50 and 100 s, 730° and 700 °C, correspondingly. Besides that thermogram 2 has features indicating a multistage burning process with several region of warming-up and attenuation. The result of interaction during this process revealed from Mossbauer spectroscopy analysis (Fig. 5a) shows that it is slightly different from the result of the 4-min activation. The difference lies in the amount of pure Fe as a quantity and particles sizes of oxide's phases (Table 1).

SEM images (Fig. 6a) of the synthesized SHS composite and the same image obtained in the characteristic radiation mode (Fig. 6b) of Fe, Zr and O showed that large Fe particles (1–3 μkm, green color) are covered with a shell-type environment, containing zirconia or mixed zirconia-iron oxide (blue). There are smaller particles between core-in-shell structures. Their composition is also mixed.

Mossbauer spectrum of the SHS composite (Fig. 5b) has shown that powder composite obtained mainly in ferromagnetic state with small addition of antiferromagnetic and paramagnetic phases. Spectrum revealed that along with Fe-component, there is a larger quantity of intermetallic well crystallized Fe_2Zr (7%) and about 2% of a solid solution of Zr(Fe). The amount of ZrO_2/Fe^{3+} component gradually increased to 5%.

Thus we envisage the following mechanisms of particles in shell formation: The exothermic thermite reaction between Zr in [Fe/Zr] composite particles and iron oxide Fe_2O_3 particles takes place in the region of burning at the surface of iron particles with formation of intermediate (mixed) oxide Zr-O-Fe. At least two possible processes of mixed oxide at the iron particle surface must be considered: (i) the interaction between iron oxide and zirconum present as a diluent in the reacting mixture, and (ii) the oxidation of an alloy or intermetallic compound between Zr and Fe formed locally at the precursor step of a synthesis. It is also possible to exclude the possibility of passing oxidation processes during cooling after propagation of the combustion wave.

4 Conclusions

Crystalline, almost spherical Fe nanoparticles were successfully synthesized and encapsulated in zirconia containing shell by self propagating synthesis on mechanically activated

powder precursors. The local structures formation at the subsequent steps of synthesis investigated by means of Mossbauer spectroscopy and SEM led to the following conclusions:

(1) Mechanical activation of 80Fe20Zr powder mixture results in formation of composite Fe particles with distribution of Zr over their volume. This allowed to reduce the activity of Zr in the mechanochemially induced reaction of Fe_2O_3 reducing in composite Fe_2O_3/[Fe/Zr] mixture with formation of highly reactive composite Fe_2O_3/[Fe/Zr] mixture with high value of contact surfaces between particles for subsequent proceeding of SHS reaction.
(2) SHS reaction proceed basically at the interfaces and at the surface of iron particles, forming the shell containing intermediate oxide of Fe and Zr.
(3) Despite multi-step procedure and complexity of the synthesis, it represents a step forward in the ability to synthesize zirconia shell on the ferromagnetic iron particles that may serve as functional protective coating regarding to particles stability and magnetic behavior.

Acknowledgements This work was supported by the Siberian Branch of the Russian Academy of Sciences, the National Academy of Science of Belarus and Moscow University Program of Development.

References

1. Sharma, S.K. (ed.): Complex Magnetic Nanostructures, vol. 201. Springer, Berlin (2009). https://doi.org/10.1007/978-3-319-52087-2
2. Kalele, S., Gosavi, S.W., Urban, J., Kulkarni, S.K.: Nanoshell particles: synthesis, properties and applications. Curr. Sci. **91**(8), 1038–1052 (2006)
3. Chaubey, G.S., Kim, J.: Structure and magnetic characterization of core-shell Fe@ZrO_2 nanoparticles synthesized by sol-gel process. Bull. Korean Chem. Soc. **28**(12), 2279–2282 (2007). https://doi.org/10.5012/bkcs.2007.28.12.227
4. Kwak, H., Chaudhuri, S.: Role of vacancy and metal doping on combustive oxidation of Zr/ZrO_2 core-shell particles. Surf. Sci. **604**, 2116–2128 (2010). https://doi.org/10.1016/j.susc.2010.09.002
5. Sarkar, A., Biswas, S.K., Pramanik, P.: Design of a new nanostructure comprising mesoporous ZrO_2 shell and magnetite core (Fe_3O_4@mZrO_2) and study of its phosphate ion separation efficiency. J. Mater. Chem. **20**, 4417–4424 (2010). https://doi.org/10.1039/b925379c/
6. Srdić, V.V., Mojić, B., Nikolić, M., Ognjanović, S.: Recent progress on synthesis of ceramics core/shell nanostructures. Process. Appl. Ceram. **7**(2), 45–62 (2013). https://doi.org/10.2298/PAC1302045S
7. Shafrir, S.N., Romanofsky, H.J., Skarlinski, M., Wang, M., Miao, Ch., Salzman, S., Chartier, T., Mici, J., Lambropoulos, J.C., Shen, R., Yang, H., Jacobs, S.D.: Zirconia-coated carbonyl-iron-particle-based magnetorheological fluid for polishing optical glasses and ceramics. Appl. Opt. **48**(35), 6797–6810 (2009). https://doi.org/10.1364/AO.48.006797
8. Shen, R., Shafrir, S.N., Miao, Ch.., Wang, M., Lambropoulos, J.C., Jacobs, S.D., Yang, H.: Synthesis and corrosion study of zirconia-coated carbonyl iron particles. J. Colloid Interface Sci. **342**, 49–56 (2010). https://doi.org/10.1016/j.jcis.2009.09.033
9. Shi, C.Y., Wang, W.-Q., Fang, J.G., Wu, J.W., Yuan, L.: The study of preparation conditions for magnetic iron zirconium co-oxide microspheres. Mater. Manuf. Process. **27**(11), 1149–1153 (2012). https://doi.org/10.1080/10426914.2011.610114
10. Kiseleva, T., Letsko, A., Talako, T., Kovaleva, S., Grigorieva, T., Novakova, A., Lyakhov, N.: Possibility of the core-in-shell iron particles formation via ma shs technology. In: Proceedings of Fourteenth Bi-National Workshop 2015 "The Optimization of the Composition, Structure and Properties of Metals, Oxides, Composites, Nano and Amorphous Materials, pp. 35–47. Ariel University (2015)
11. Rogachev, A.S., Mukas'yan, A.S.: Burning of heterogeneous nanostructured systems. Fiz. Goreniya Vzryva (in Russian) **46**(3), 3–30 (2010)

12. Lyakhov, N.Z., Talako, T.L., Grigor'eva, T.F.: In: Lomovskii, O.I. (ed.) Mechanoactivation Effect in Phase- and Structure Formation Processes under Self-Propagating High-Temperature Synthesis. Parallel', Novosibirsk (2008) [in Russian]
13. Grigor'eva, T.F., Letsko, A.I., Talako, T.L., Tsybulya, S.V., Vorsina, I.A., Barinova, A.P., Il'yushchenko, A.F., Lyakhov, N.Z.: The way to produce Cu/ZrO_2 composites by combining mechanical activation and self-propagating high-temperature synthesis. Combust. Explos. Shock Waves **47**, 174 (2011). https://doi.org/10.1134/S001050821
14. Grigor'eva, T.F., Letsko, A.I., Talako, T.L., Tsybulya, S.V., Vorsina, I.A., Barinova, A.P., Il'yushchenko, A.F., Lyakhov, N.Z.: The way to produce Cu/TiO_2 composites by combining mechanical activation and self-propagating high-temperature synthesis. Russ. J. Appl. Chem. **84**(11), 1765–1768 (2011). https://doi.org/10.1134/S1070427211110024
15. Kiseleva, T.Yu., Letsko, A.I., Talako, T.L., Griroryeva, T.F., Novakova, A.A., Lyakhov, N.Z.: Mechanochemically synthesized powder precursors local structure influence on the microstructure of SHS @ composites. Nanotechnol. Russ. **10**, 220–230 (2015). https://doi.org/10.1134/S1995078015020123
16. Kiseleva, Y., Novakova, A.: Mossbauer spectroscopy in the technology of nanocomposite functional materials. Bull. Russ. Acad. Sci. Phys. **79**(8), 1002–1007 (2015). https://doi.org/10.3103/S1062873815080122
17. Konygin, G.N., Stevulova, N., Dorofeev, G.A., Elsukov, E.P.: Effect of crushing bodies onto results of mechanical alloying of Fe and Si powders mixtures. Khim. Interes. Ustoich. Razvit. **10**(1–2), 119–126 (2002)
18. Schneider, C.A., Rasband, W.S., Eliceiri, K.W.: NIH Image to ImageJ: 25 years of image analysis. Nat. Methods **9**(7), 671–675 (2012). https://doi.org/10.1038/nmeth.2089
19. Bruggemann, S.A., Artzybashev, Y.A., Orlov, S.V.: (UNIVEM) Version 2.07 (2001–2003)
20. Lyakishev, N.P. (ed.): State Diagrams for Double Metallic Systems. Mashinostroenie, Moscow (1996). [in Russian]
21. Del Bianko, L., Hernando, A., Bonetti, E.: Grainboundary structure and magnetic behavior in nanocrystalline ball-milled iron. Phys. Rev. B **56**(14), 8894–8901 (1997). https://doi.org/10.1103/PhysRevB.56.8894
22. Gleiter, H.: Materials with ultrafine microstructures: retrospectives and perspectives. Nanostruct. Mater. **1**, 1–19 (1992). https://doi.org/10.1016/0965-9773(92)90045-Y
23. Novakova, A.A., Agladze, O.V., Kiseleva, T. Yu.., Tarasov, B.P., Perov, N.S.: The grain boundary structure influence n the magnetic properties of nanocrystalline iron. Bull. Russ. Acad. Sci. Phys. **65**(7), 1016–1021 (2001)
24. Kim, H.S., Estrin, Y., Bush, M.B.: Plastic deformation behaviour of fine-grained materials. Acta Mater. **48**(2), 493–504 (2000). https://doi.org/10.1016/S1359-6454(99)00353-5
25. Weiss, B.Z., Bamberger, M., Stupel, M.M.: Phase transformation in the Zr-rich part of the Zr-Fe system resulting from heat treatment and plastic deformation. Metall. Trans. A. **18A**, 27–33 (1987). https://doi.org/10.1007/BF02646218
26. Filippov, V.P.: Potentialities of Mossbauer spectroscopy for studying zirconium alloys and their oxide films. Met. Sci. Heat Treat. **45**(11–12), 452–460 (2003)
27. Filippov, V.P., Bateev, A.B., Lauer, Yu.A.., Kargin N.I.: Mossbauer spectroscopy of zirconium alloys. Hyperfine Interact. **217**, 45–55 (2013). https://doi.org/10.1007/s10751-012-0747-8
28. Lomovskii, O.I. (ed.): Mechanocomposites Precursors for Creating Materials with New Properties,. Siberian Branch RAS, Novosibirsk (2010) [in Russian]
29. Kiseleva, T.Y., Novakova, A.A., Chistyakova, M.I., Polyakov, A.O., Gendler, T.S., Grigorieva, T.F.: Iron-based amorphous magnetic phase formation in the course of Fe and F_2O_3 mechanical activation. Diffus. Defect Data Part B: Solid State Phenom. **152**, 25–28 (2009). https://doi.org/10.4028/www.scientific.net/SSP.152-153.25
30. Grigor'eva, T.F., Barinova, A.P., Lyakhov, N.Z.: Mechanochamical Synthesis in Metallic Systems. Parallel', Novosibirsk (2008) [in Russian]
31. Kiseleva, T.Yu., Novakova, A.A., Grigor'eva, T.F., Barinova, A.P., Vorsina, I.A.: Mechanical synthesis for corundum ceramics/intermetallide nanocomposites. Adv. Mater. (Russ.) **6**, 11–20 (2008)
32. Kiseleva, T., Novakova, A., Zimina, M., Polyakov, S., Levin, E., Grigoryeva, T.: Mechanochemically induced formation of amorphous phase at oxide nanocomposite interfaces. J. Phys.: Conf. Ser. **217**(1), 012106–012106 (2010). https://doi.org/10.1088/1742-659,6/217/1/012106
33. Stefanic, G., Music, S., Gajovic, A.: Structural and microstructural changes in monoclinic ZrO_2 during ball milling with stainless steel assembly. Mater. Res. Bull. **41**, 764–777 (2006). https://doi.org/10.1016/j.materresbull.2005.10.006
34. Jiang, J.Z., Poulsen, F.W., Morup, S.: Structure and thermal stability of nanostructured iron-doped zirconia prepared by high energy ball milling. J. Mater. Res. **14**(4), 1343–1452 (1999). https://doi.org/10.1557/JMR.1999.0183